

Process Raman as a comprehensive solution for downstream buffer workflow

Authors

Michelle Nolasco¹

Andrew Siemers¹

Kristina Pleitt¹, Ph.D.

Nimesh Khadka², Ph.D.

¹BioProduction Group, ThermoFisher Scientific, St. Louis, Missouri USA

²Analytical Instrument Group, ThermoFisher Scientific, Tewksbury, Massachusetts USA

Industry/Application:

Biopharma PAT / Downstream

Products used:

Thermo Scientific™ MarqMetrix™ All-In-One Process Raman Analyzer, Thermo Scientific™ MarqMetrix™ FlowCell Sampling Optic, Thermo Scientific™ MarqMetrix™ BallProbe™ Sampling Optic

Goals:

Enabling real-time excipient quantification and quality assessment using process Raman

Key Analytes:

Arginine, Histidine, Sucrose

Key Benefits:

- Enables real-time excipient quantification with cost and time benefits from eliminating the need for laboratory analytics
- Provides a platform to take actionable decision using real time data rather than theoretical estimation.
- Demonstrates potential of process Raman as a PAT tool for automation of Ultrafiltration/Diafiltration (UF/DF) and other downstream processes through simultaneous and real-time monitoring, quality assessment, and allowing multimodal feedback controls.

Introduction

Raman technology is rapidly gaining interest as a promising Process Analytical Technology (PAT) solution for real-time, non-invasive monitoring and control of downstream biopharma processes, especially for therapeutics like monoclonal antibodies (mAbs) and nucleic acids. Raman measurement, based on the vibration of molecular bonds, is highly specific for identification and quantification, even in complex or interfering matrices.

As an in-line PAT tool, Raman spectroscopy offers direct and rapid measurement in aqueous phases without sample preparation. These features make it ideal for monitoring and controlling dynamic processes such as downstream processing.

This study demonstrates a real-time methodology for accurately quantifying formulation excipients in the dynamic ultrafiltration/diafiltration (UF/DF) process using the Thermo Scientific™ MarqMetrix™ All-In-One Process Raman Analyzer (Figure 1). In addition, this study also illustrates a case where process Raman was able to provide real-time information on buffer quality.

Experimental details

Excipient quantification models

Calibration samples with defined concentrations of L-histidine, L-arginine, and sucrose were prepared using a design of experiments (DoE) approach called Uniform Design (UD) derived from number theory.¹ UD significantly reduces the total number of experiments while optimally spans the whole process space for model building and validation. These excipients were chosen due to their relevance in high-concentration monoclonal antibody (mAb) formulations. The analyte concentrations in the mixtures were designed with UD, with ranges of L-histidine (0-15 mg/mL), L-arginine (0-40 mg/mL), and sucrose (0-200 mg/mL) to develop calibration models. Each sample was passed in randomized order through a FlowCell Probe integrated with the MarqMetrix All-In-One Process Raman Analyzer at a flow rate of 100 mL/min. The acquisition parameters were set to a laser power of 450 mW, an integration time of 3000 ms, and an average of 3 spectra, resulting in an 18 second total collection time per spectrum.

A Partial Least Squares (PLS) chemometric model was developed using the spectral range of 800 to 3235 cm^{-1} Raman shift. The spectra were normalized using infinity norm calculated in the spectral region of 2900 to 3230 cm^{-1} and preprocessed with a Savitzky-Golay (SavGol) filter (1st derivative, polynomial order = 2, window width = 13) and mean-centered. Overfitting was minimized by selecting appropriate latent variables using a leave-one-out cross-validation (LOOCV) strategy. To initially validate the model performance, seven different validation samples were collected in three different instruments using the same acquisition parameters as used in training data acquisition.

To allow the generalization of these excipient models to their use in ultrafiltration/diafiltration (UF/DF) process for IgG1 mAb, Raman spectra for IgG1 mAb (5 to 150 mg/mL in various matrices) were added to the training dataset, and new models were developed. The addition of these protein spectra allowed the resulting PLS model to better distinguish Raman signals among L-arginine, L-histidine, and protein.

Ultrafiltration/Diafiltration process

The Raman Process Analyzer with FlowCell Probe was integrated in-line to monitor an UF/DF process (Figure 2). A PES membrane was equilibrated with tris buffer pH 7.0 prior to feeding a purified IgG1 mAb at 10 g/L to a target loading of 500 g/m². In the first ultrafiltration (UF) step, the mAb was concentrated at feed rate of 300 L/m²/hr, and TMP was maintained between 10-15 psi via manual flow restrictor. The mAb was then buffer exchanged into final formulation matrix containing L-histidine, L-arginine, and sucrose by manually feeding in the diafiltration (DF) buffer to the recirculation tank to maintain constant volume. After buffer exchange, the mAb was further concentrated to the desired final concentration in the second UF step.

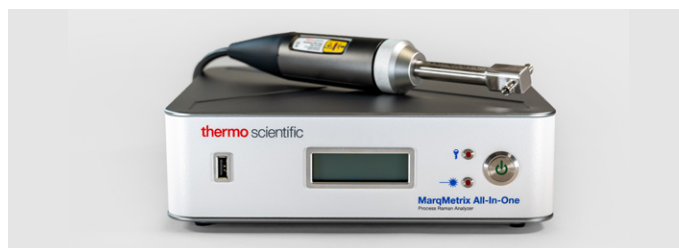


Figure 1. Thermo Scientific MarqMetrix All-In-One Process Raman Analyzer, Thermo Scientific MarqMetrix FlowCell Sampling Optic.

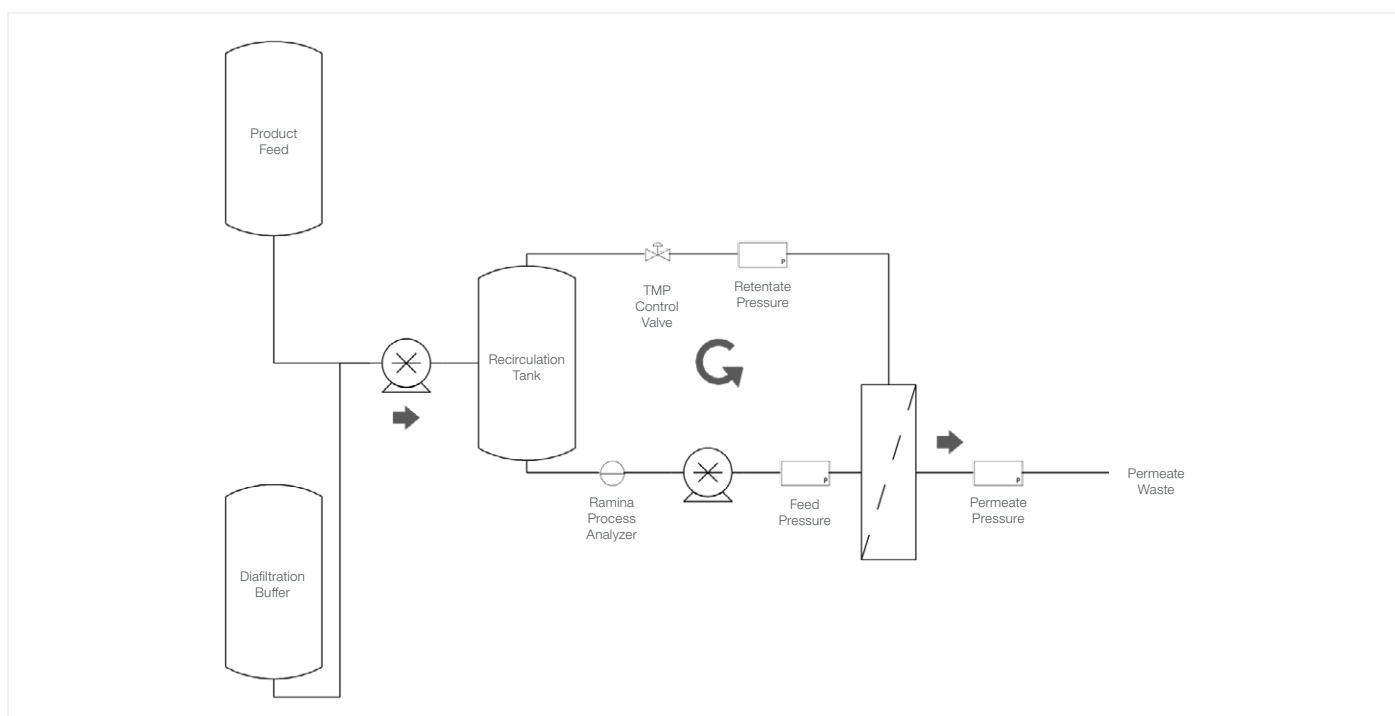


Figure 2. Ultrafiltration/Diafiltration (UF/DF) Process Diagram.

Buffer stability

Buffers in downstream processes are often prepared in advance and typically used based on prior knowledge of their stability, rather than confirming stability through analytical analyses before each UF/DF run. In two of our downstream runs, we noticed that the process Raman spectroscopy predicted a lower-than-expected sucrose concentration in the excipient buffer. To mitigate potential risks, we discarded the previously prepared buffer and made a fresh batch. The predictions from process Raman analyzer on the new buffer were much closer to the reference values obtained from HPLC (high performance liquid chromatography). To further validate this capability in a controlled experiment, we measured the Raman spectra of the excipient buffer, which contains L-histidine, L-arginine, and sucrose, at room temperature for 15 days. The buffer was monitored through a Thermo Scientific MarqMetrix BallProbe Sampling Optic integrated with the MarqMetrix All-In-One Process Raman Analyzer. The acquisition parameters were set to a laser power of 450 mW, an integration time of 3000 ms, and an average of 3 spectra, resulting in an 18 second total collection time per spectrum. Additionally, we collected data on pH, osmolarity, and performed HPLC analysis at various time intervals.

Results

The Partial Least Squares (PLS) models for L-histidine, L-arginine, and sucrose were initially tested using seven independent samples collected on three different process Raman analyzers. Data were mathematically processed to standardize spectra across instruments before applying the models. All the spectra were interpolated to have a common x-axis by equally spacing the 2048 pixels across 60 to 3250 cm^{-1} Raman shift, followed by relative y-axis standardization using the SRM fluorescence data as described in the NIST standardization protocol.² Figure 3 shows the correlation plot of predicted versus reference values for L-histidine, L-arginine, and sucrose for the validation samples. A correlation coefficient of over 95% and a root means square error (RMSE) of less than 5% of the reference value for calibration, cross-validation, and prediction across three instruments demonstrate the reliability of process Raman to accurately predict the concentrations of these excipients, as well as easy model transferability.

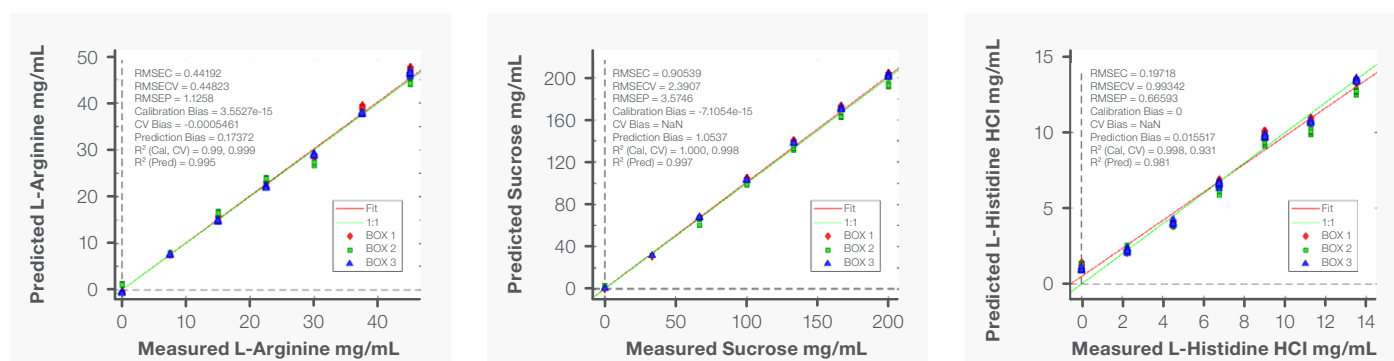


Figure 3. Correlation plot of predicted vs reference values for L-histidine, L-arginine, and sucrose across three different instruments.

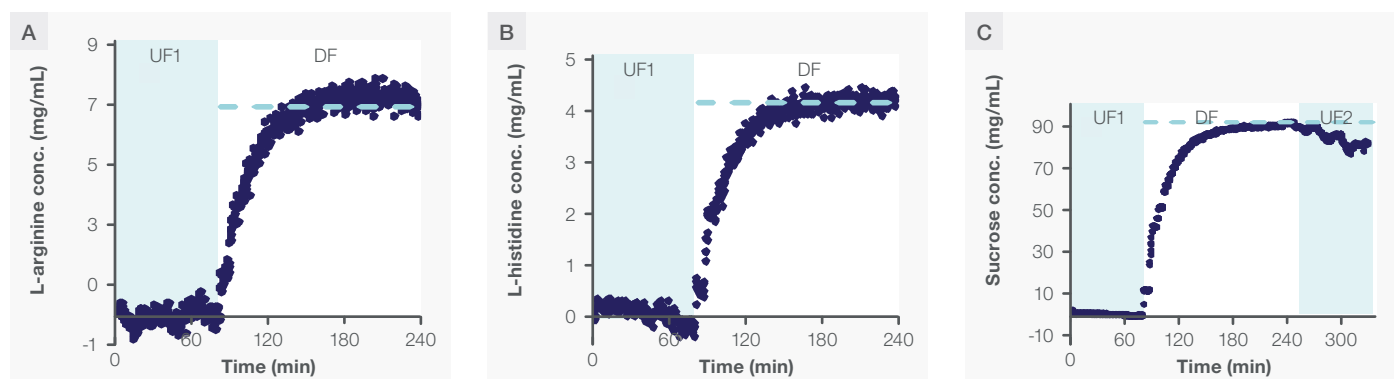


Figure 4. Raman concentration predictions during bench-scale UF/DF of IgG1 mAb for L-arginine (A), L-histidine (B), and sucrose (C); target end conc. shown with light blue dashed line.

The L-histidine, L-arginine, and sucrose models were then applied to the data acquired during the ultrafiltration/diafiltration (UF/DF) process. The predicted values for L-histidine, L-arginine, and sucrose are shown in Figures 4A, 4B, and 4C, respectively. The average predicted concentrations of L-histidine, L-arginine, and sucrose at the end of buffer exchange were compared to the reference values, resulting in a prediction error of less than 5% of the reference values (Table 3). This clearly illustrates the capability of process Raman analyzers to monitor and quantify excipients in real-time.

The real-time prediction of sucrose concentrations over 15 days at room temperature in a briefly air-exposed formulation buffer, containing L-histidine, L-arginine, and sucrose, is shown in Figure 5A. This scenario mimics what may occur during the storage of the formulation buffer. Initially, the predicted sucrose concentration was 86 mg/mL and remained stable for 5 days, but then steadily decreased to 57 mg/mL by day 15. Predictions from the arginine and histidine PLS models behaved similarly to those from the sucrose model, showing accurate and stable values up to day 5, but then steadily increasing until day 15 (data not shown). Raman spectral analysis revealed that the decrease in the sucrose peak was accompanied by the appearance of glucose and fructose Raman peaks (Figures 5B and 5C). HPLC analysis confirmed the intactness of arginine and histidine for all 15 days, and the hydrolysis of sucrose into glucose and fructose (Figures 5D and 5E).

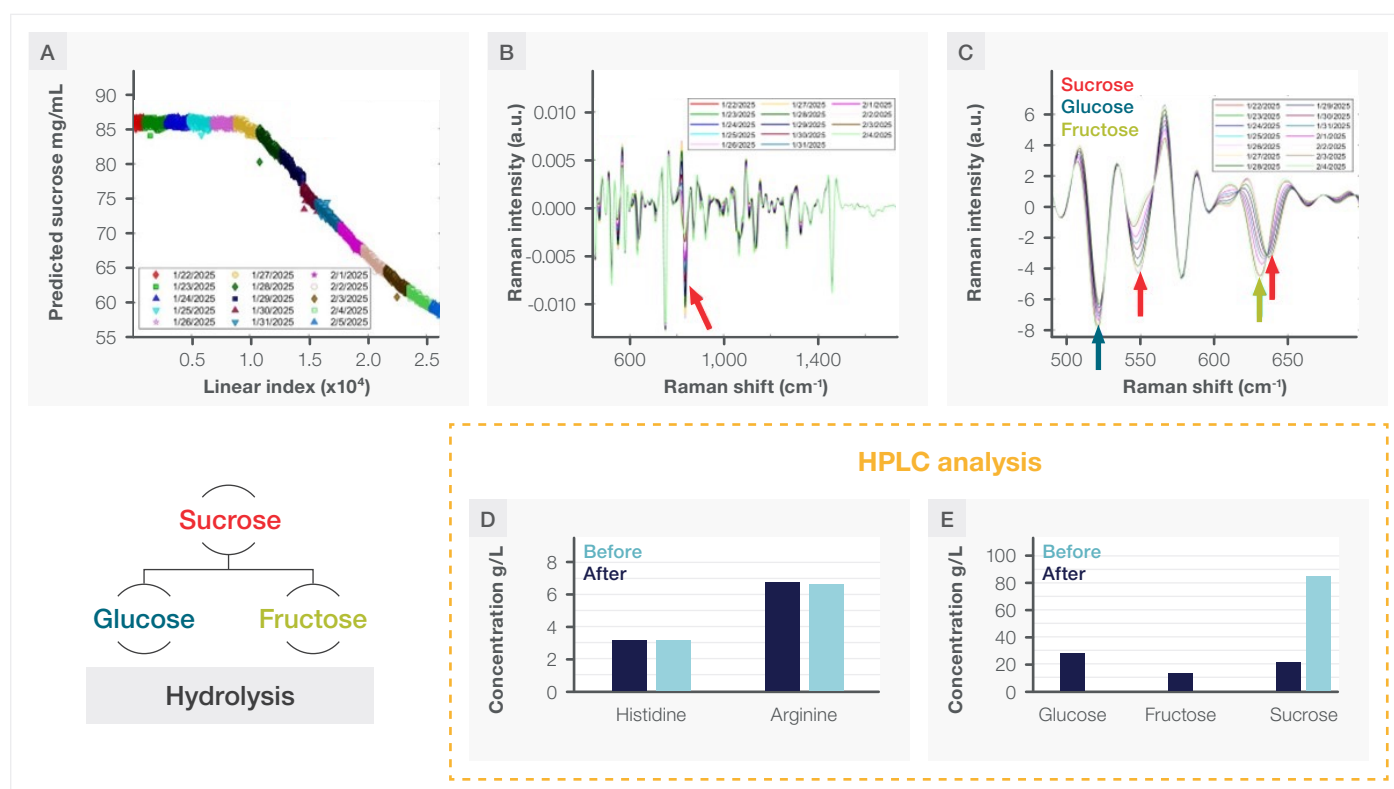


Figure 5. Showing the sucrose prediction over 14 days (A). Initially, the sucrose concentration was 86 mg/mL that lowered to about 57 mg/mL over the span of 14 days. The decrease in sucrose prediction were evident by decrease in sucrose specific intensity of 835 cm^{-1} that is assigned to the twisting ($\tau(\text{CH}_2)$) with some contribution from symmetric stretching ($\nu(\text{CC})$) vibrational mode (B). Showing in figure C, the decrease in sucrose specific band (red arrow; $\sim 550 \text{ cm}^{-1}$ assigned as in-plane bending ($\beta(\text{OCO})$) is followed by increase in glucose (blue; $\sim 525 \text{ cm}^{-1}$) and fructose (green; $\sim 640 \text{ cm}^{-1}$) specific Raman band that are assigned mainly to the deformation of CCC, CCO, and OCO bands. In figure D and E the result of day 1 (Before; blue) and day 15 (After; cyan) are compared where arginine and histidine remained unchanged while sucrose hydrolyzed to glucose and fructose.

Excipient	Reference concentration (g/L)	Predicted concentration (g/L)	% absolute error
L-histidine	4.2	4.1	1.0
L-arginine	7.0	7.1	1.4
Sucrose	92.4	95.6	3.4

Table 3. Prediction Error Calculation.

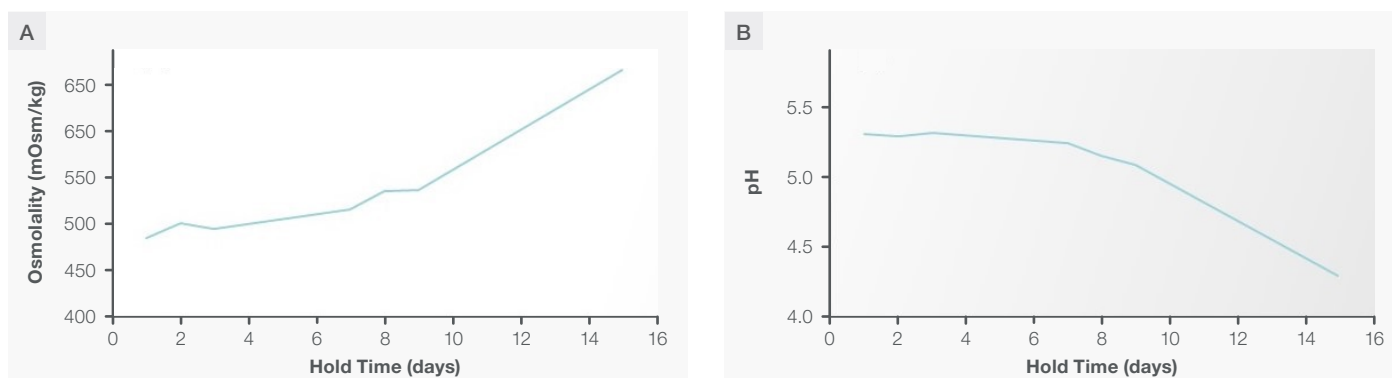


Figure 6. Showing increase in osmolarity by 40% (A) and decrease in pH by 1 unit during the hold period (B).

Acidic hydrolysis of sucrose is well documented in the literature.³ To investigate if the root cause had pH-association, we examined the osmolarity and pH profiles during the experiment (Figures 6A and 6B). The onset of sucrose hydrolysis coincided with an increase in osmolarity and a decrease in pH, suggesting that the hydrolysis of sucrose into glucose and fructose is most likely driven by the lower pH. Since no acid was added to the system, the pH decrease was likely due to external factors. Although we did not identify the exact cause of the pH decrease, potential factors in practice could include bacterial growth, improper pH adjustment during buffer preparation, or dissolution of carbon dioxide or other acid-producing gases, among others.

Note that the sucrose PLS model was developed using a mixture of L-histidine, L-arginine, sucrose, and protein, and lacks any spectral information from glucose and fructose. Since glucose and fructose have significant overlaps in a wide spectral region, this explains why the Raman predictions were higher compared to the reference HPLC values.⁴ The same reasoning applies to the discrepancies observed in Raman predictions for L-arginine and L-histidine (data not shown) when compared to the HPLC values (Figure 5D). In both cases, predictions can be improved by augmenting the model with additional training data that includes glucose and fructose spectral information. However, this was beyond the scope of the current work.

Not including glucose and fructose spectral information in the models is advantageous for monitoring buffer quality. As glucose and fructose are produced by sucrose hydrolysis, new spectral features appear that were not present in the training dataset. The Q residual is one of the model statistics calculated using the residual spectra remaining after projecting the original spectra into the model space.⁵ As the spectral information of glucose and fructose increases with the progress of sucrose hydrolysis, the magnitude of the Q residual increases over time, as shown in Figure 7. Users can leverage this information to design quality control measures based on the reduced Q vs. T^2 plot to assess buffer quality.⁵ For instance, in this study, a mean value of 0.15 for the reduced Hotelling T^2 and 0.5 for the reduced Q residual, with 95% confidence intervals for upper and lower limits (red dotted oval in Figure 7), can be used as quality control thresholds. Any buffer with reduced Q and T^2 values beyond these limits is deemed to fail quality control. All spectra after day 5 had low reduced T^2 and high reduced Q values, thus failing the quality control.

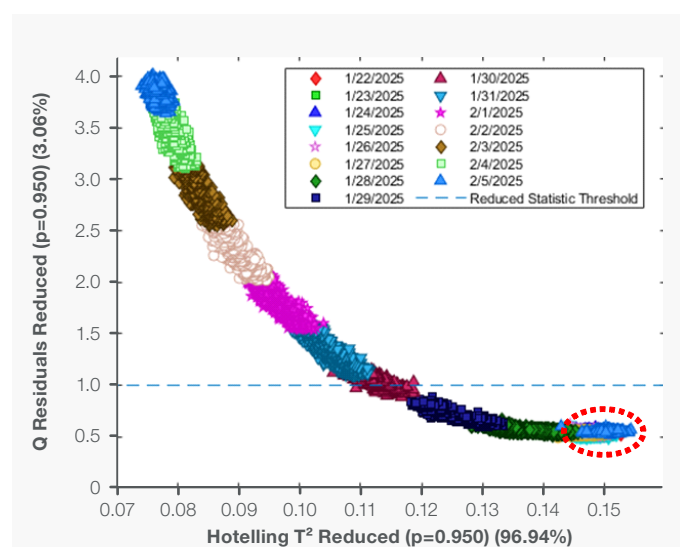


Figure 7. Showing increase in Q residual with sucrose hydrolysis, calculated by projecting the Raman data into the PLS sucrose model. The red dotted oval showing one of the possible control limits for quality assessment.

Conclusion

1. Real-time quantification of L-arginine, L-histidine, and sucrose were demonstrated with absolute error of < 5% in a UF/DF process using process Raman analyzer configured with FlowCell probe. In absence of in-line PAT tools to quantify these excipients, the volume needed for diafiltration (V_{df}) is carried out based on following mathematical expression:

$$V_{df} = V_0 * D = V_0 * \ln(C_0 / C_f) / \ln(1-R)$$

Equation 1.

where:

- V_0 is the initial volume of the solution.
- D is the number of diavolumes required.
- R is retention factor
- C_0 is initial concentration of solute
- C_f is the final concentration of solute

In practice, the retention factor for excipients is typically assumed to be 0, as the pore size of the diafiltration membrane is significantly larger than the hydrodynamic size of excipients. However, charge buildup across the membrane results in electrochemical potential which in turn prevents the free mobility of charged excipients, thereby increasing their retention factor above 0. This effect is known as the Gibbs-Donnan effect.⁶ In such scenarios, the empirically calculated volume needed for diafiltration (V_{df}) can result in incomplete buffer exchange, which may affect the functionality and stability of monoclonal antibodies (mAbs). An in-line process Raman analyzer provides a reliable solution to this issue by offering real-time monitoring of excipient concentrations. This enables tighter process control and ensures product quality by allowing for immediate adjustments to the diafiltration process, thereby preventing incomplete buffer exchange and maintaining the stability and functionality of the therapeutic product.

Similarly, in Figure 4C, the sucrose concentration in the retentate decreased during UF2, as confirmed by offline HPLC analysis. Given the hydrodynamic size of sucrose relative to the pore size of the membrane, sucrose should theoretically exchange freely between the retentate and filtrate, resulting in equal concentrations in both. However, as the protein concentration increases, the osmotic pressure also rises, making the exclusion of water thermodynamically unfavorable.

To balance the osmotic pressure difference, *sucrose is excluded along with water*.⁶ This effect was accurately captured in the real-time predicted data from the process Raman analyzer. Thus, process Raman provides unique capabilities to ensure product quality by offering real-time data, rather than relying on empirical hypotheses.

2. This work, combined with our previous demonstrations of accurate in-line protein quantification during UF/DF processes,^{7,8} clearly highlights the value of process Raman for downstream process monitoring. Raman spectroscopy allows for the simultaneous measurement of multiple critical process parameters (CPPs) with a single scan. These findings establish process Raman as a PAT tool with unparalleled benefits compared to other analytical methods.
3. Simultaneous measurement of protein and excipient concentrations not only allows tighter process control but also opens opportunities for automating downstream processing.
4. The ability of process Raman to provide real-time insights into buffer quality before its use in UF/DF runs offers substantial value by preventing batch failures. This capability enhances quality control, making Raman spectroscopy an essential tool for integration as an in-line sensor to improve downstream process monitoring, control, and automation.

References

1. Zhang, L.; Liang, Y.-Z.; Jiang, J.-H.; Yu, R.-Q.; Fang, K.-T. Uniform Design Applied to Nonlinear Multivariate Calibration by ANN. *Analytica Chimica Acta* **1998**, 370 (1), 65–77. [https://doi.org/10.1016/S0003-2670\(98\)00256-6](https://doi.org/10.1016/S0003-2670(98)00256-6).
2. Choquette, S. J.; Etz, E. S.; Hurst, W. S.; Blackburn, D. H.; Leigh, S. D. Relative Intensity Correction of Raman Spectrometers: NIST SRMs 2241 through 2243 for 785 Nm, 532 Nm, and 488 Nm/514.5 Nm Excitation. *Appl Spectrosc* **2007**, 61 (2), 117–129. <https://doi.org/10.1366/000370207779947585>.
3. Torres, A. P.; Oliveira, F. a. r.; Silva, C. I. m.; Fortuna, S. p. THE INFLUENCE of pH ON the KINETICS of ACID HYDROLYSIS of SUCROSE. *Journal of Food Process Engineering* **1994**, 17 (2), 191–208. <https://doi.org/10.1111/j.1745-4530.1994.tb00335.x>.
4. Wiercigroch, E.; Szafraniec, E.; Czamara, K.; Pacia, M. Z.; Majzner, K.; Kochan, K.; Kaczor, A.; Baranska, M.; Malek, K. Raman and Infrared Spectroscopy of Carbohydrates: A Review. *Spectrochimica Acta Part A: Molecular and Biomolecular Spectroscopy* **2017**, 185, 317–335. <https://doi.org/10.1016/j.saa.2017.05.045>.
5. Kumar, S.; Martin, E. B.; Morris, J. DETECTION OF PROCESS MODEL CHANGE IN PLS BASED PERFORMANCE MONITORING. *IFAC Proceedings Volumes* **2002**, 35 (1), 125–130. <https://doi.org/10.3182/20020721-6-ES-1901.00752>.
6. Agrawal, P.; Wilkstein, K.; Guinn, E.; Mason, M.; Serrano Martinez, C. I.; Saylae, J. A Review of Tangential Flow Filtration: Process Development and Applications in the Pharmaceutical Industry. *Org. Process Res. Dev.* **2023**, 27 (4), 571–591. <https://doi.org/10.1021/acs.oprd.2c00291>.
7. Nolasco, M.; Pleitt, K.; Khadka, N. Using a Process Raman Analyzer as an In-Line Tool for Accurate Protein Quantification in Downstream Processes.
8. Nolasco, M.; Pleitt, K.; Khadka, N. Raman-Based Accurate Protein Quantification in a Matrix That Interferes with UV-Vis Measurement.

Learn more at thermofisher.com

thermo scientific